Journal of Alloys and Compounds 509 (2011) 6942–6945

Contents lists available at ScienceDirect

Journal of Alloys and Compounds

journal homepage: www.elsevier.com/locate/jallcom

Catalyst-free synthesis of ZnO microrod arrays on SiC substrate and their tunable photoluminescence by erosion process

Kaixing Zhu[a], Wenjun Wang[a,*], Xiaolong Chen[a], Jun Liu[a], Bo Song[b], Liangbao Jiang[a], Jiangang Guo[a], Jinyang Cheng[c]

[a] *Beijing National Laboratory for Condensed Matter Physics, Institute of Physics, Chinese Academy of Sciences, P.O. Box 603, Beijing 100190, China*
[b] *Center for Composite Materials, Harbin Institute of Technology, Harbin 150080, China*
[c] *Beihang University, XueYuan Road No. 37, Haidian District, Beijing 100191, China*

ARTICLE INFO

Article history:
Received 22 December 2010
Received in revised form 4 March 2011
Accepted 1 April 2011
Available online 8 April 2011

Keywords:
Semiconducting materials
ZnO
Microrod
Photoluminescence

ABSTRACT

We present here the results on the preparation and characterization of highly oriented ZnO microrods fabricated on SiC substrate via a vapor solid route. These ZnO microrods grow along the *c*-axis perpendicularly to the substrate and are well separated from each other. Photoluminescence (PL) due to the band-gap emission (centered at 380 nm) and defect-related deep band emission (centered at 530 nm) were observed. Tunable PL intensities of these two bands were achieved by acid etching for varying durations.

1. Introduction

Recently, one-dimensional (1D) ZnO micro/nano-structures such as wires, rods, tubes have drawn much research interest because of their potential capabilities in constructing novel electrical and optical devices [1,2]. Large scaled and highly oriented micro/nano-structures are highly desirable for both research studies and industrial applications. Many attempts have been reported for the synthesis of arrayed ZnO micro- or nano-structures. Oriented ZnO microtubes and microrods have been prepared by aqueous thermal decomposition of Zn^{2+} amino complex [3,4]. Well aligned vertical ZnO nanopillars were fabricated by epitaxial electrodeposition [5] and wet chemical deposition [6]. Growing of ordered ZnO nanowire or nanorod arrays were demonstrated by using nanosphere lithography [7–9] and electron beam lithography [10,11]. However, these available methods usually refer to complicated preparation procedure [10–14] or introduce foreign metal catalysts (such as Au, Co, etc.) [15–18]. Therefore, a catalyst-free synthesis of well oriented ZnO arrays via a facile way is still highly desired. In addition, tuning photoluminescence (PL) properties, including changing luminescent peak position and peak intensity, has been a hot topic for its potential applications in multiplexed labeling [19–21], biological sensing [22,23] and light-emitting displaying [24]. Visible PL in ZnO is interesting since it has potential applications for cell labeling [25]. Besides, the defect related visible emission can be needed to generate white light in low voltage field emission displays. Many techniques have been presented to tune PL such as element doping [26], size altering [27,28], and polymer bonding [19], yet much more convenient method needs to be developed to meet industrial need.

In this paper, we present a facile technique for fabrication of highly oriented ZnO microrod arrays by chemical vapor deposition (CVD) method on 6H–SiC substrate without using any catalyst. PL results indicate that there exist two emission bands located at UV and visible wavelengths which correspond to the band-gap and defect-related emission, respectively. The PL intensities can be tuned by acid etching which provides useful information for optical applications of ZnO material.

2. Experimental

The growth process was carried out in a quartz tube, which was located in the central of a conventional horizontal furnace [29]. In a typical procedure, a mixture of ZnO and graphite powders in a certain ratio (1:1 by weight) was loaded in an alumina boat which was then placed in the central heating zone of the quartz tube. 6H–SiC substrate, having been ultrasonically cleaned with deionized water and ethanol before, was then put 5 mm downstream to collect products. The quartz tube was pumped mechanically and then purged with argon to clean away the traces of impurity gases. After repeating this procedure three times, the tube was heated to 990 °C in 60 min under an argon flow of 20 sccm (standard cubic centimeters per minute). Oxygen with a flow rate of 2 sccm was introduced when the temperature reached 990 °C while keeping argon flow rate remaining constant. Then the system

---

* Corresponding author. Tel.: +86 010 82649032; fax: +86 010 82649646.
E-mail address: wjwang@aphy.iphy.ac.cn (W. Wang).

0925-8388/$ – see front matter © 2011 Elsevier B.V. All rights reserved.
doi:10.1016/j.jallcom.2011.04.007

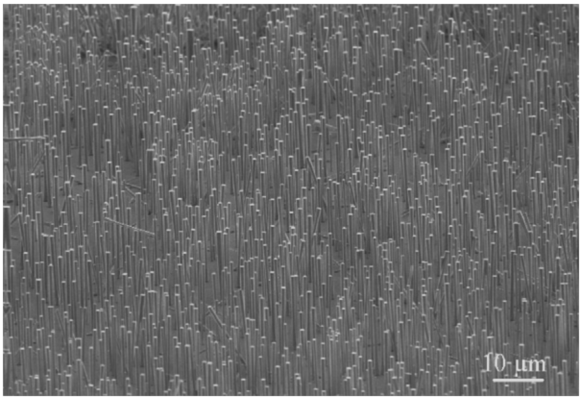

Fig. 1. Scanning electron microscope image of the aligned ZnO microrod arrays in a tilted view.

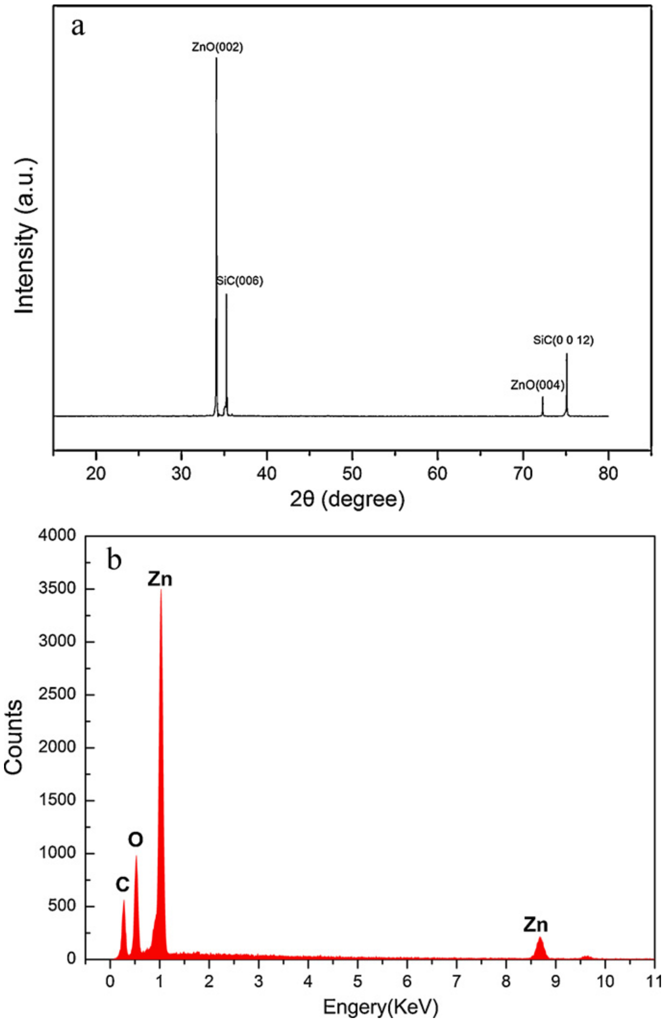

Fig. 2. (a) X-ray diffraction patterns and (b) EDX spectra of the products.

temperature was kept at 990 °C for 40 min. The power was shut off and the furnace was cooled down to room temperature. Then, a thin layer of white product was obtained on the 6H–SiC substrate. Tartaric acid with a concentration of 0.3 mM was used to corrode the obtained product at room temperature for 9, 13 and 16 h, respectively.

The obtained product was characterized by using X-ray powder diffraction (XRD), field emission scanning electron microscopy (SEM), energy-dispersive X-ray spectroscopy (EDX) and high-resolution transmission electron microscopy (HRTEM). The PL properties were characterized using He–Cd laser with an excitation wavelength of 325 nm at room temperature.

3. Results and discussion

Fig. 1 is the SEM image of the as-grown ZnO microrod arrays in a tilted view in which the uniform morphology and well alignment features were shown clearly. The majority of the products have a diameter of 0.5–1.5 μm and an approximate length of 50 μm. EDX (Fig. 2a) shows that the products consist of zinc and oxygen element. In XRD pattern (Fig. 2b), two main peaks located at $\sim$34.3° and $\sim$72.6° correspond to (0 0 2) and (0 0 4) peak of the wurtzite ZnO, respectively. This indicates that the *c*-axis of the microrods was perpendicular to the substrate surface, which is in good accordance with SEM image as shown in Fig. 1. Besides ZnO peaks, two more peaks at $\sim$35.5° and 75.2° which can be assigned to the 6H–SiC substrate (0 0 6) and (0 0 1 2) planes, respectively. In order to further gain the information of the crystal structure, TEM analysis was performed. Fig. 3a is a TEM image of a microrod removed from the arrays which shows uniform diameter along the stem. HRTEM (Fig. 3b) recorded from the same microrod in Fig. 3a indicates that the microrod is of single-crystalline nature and grows along [0 0 0 1] direction. According to the experimental results, we proposed the growth mechanism for the highly oriented ZnO microrod arrays as following. The initial products of zinc reacting with oxygen are

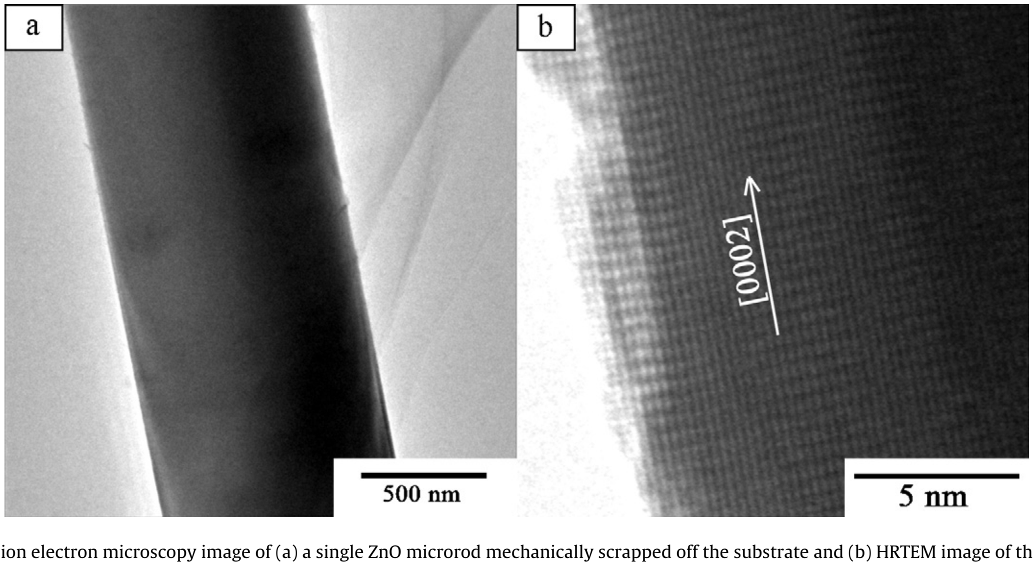

Fig. 3. Transmission electron microscopy image of (a) a single ZnO microrod mechanically scrapped off the substrate and (b) HRTEM image of the same microrod.

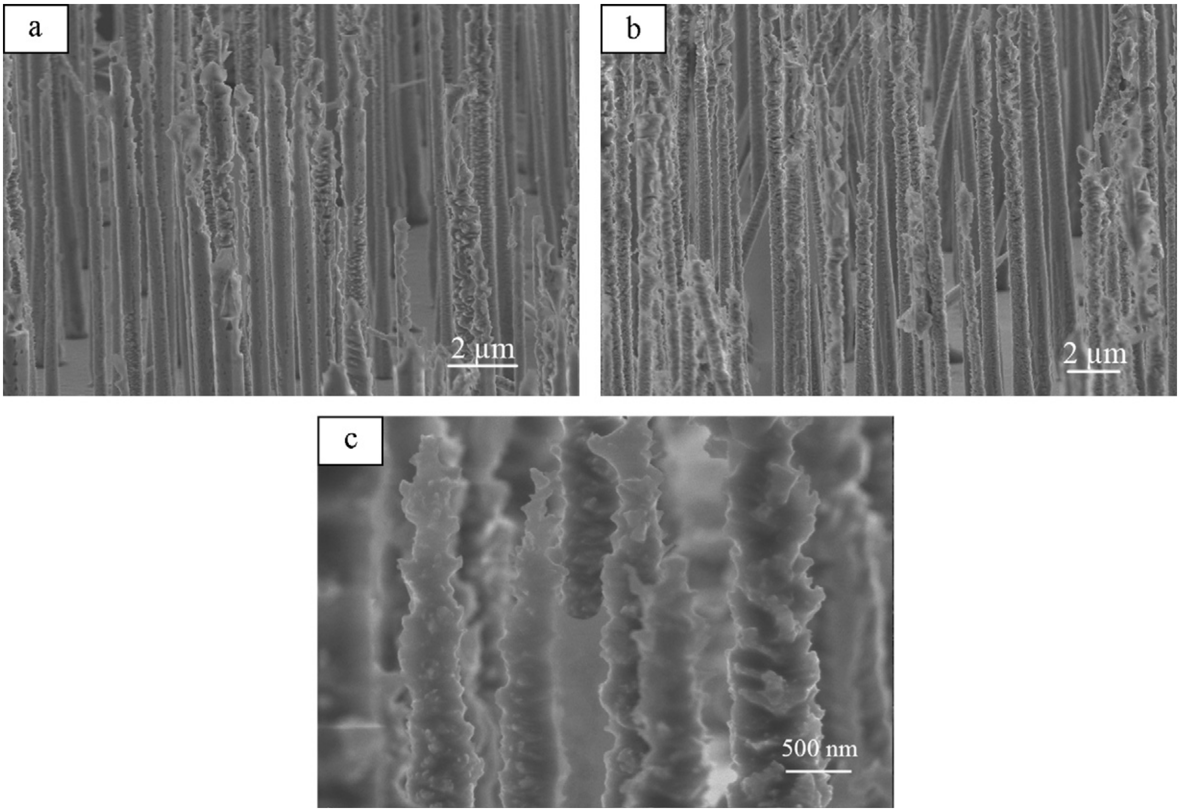

Fig. 4. SEM images of ZnO microrod arrays after acid erosion for 9 h (a), 13 h (b) and 16 h (c).

suboxides (ZnO_x, $x < 1$) because of the deficient amount of oxygen in the tube. Since Zn and ZnO_x ($x < 1$) have low melting temperature, they should be in vapor phases at high temperature zone. Then, these vapor phase species can be carried by the argon onto the SiC substrate to form liquid droplets randomly, which provide idea adsorption site for zinc and oxygen atoms. Due to the lattice match with SiC substrate and the growth habits that ZnO growing along [0 0 0 1] direction occurs faster than growing in prismatic directions [30,31], one dimensional ZnO microrods along [0 0 0 1] were formed consequently. Fig. 4 illustrates the SEM images of the acid etched ZnO microrod arrays. It can be noted that the surfaces of the microrod arrays become rougher and the diameters become thinner as etching duration extends from 9 h to 16 h, clearly shown in Fig. 4a–c. Furthermore, the upper part of the arrays was corroded more severe than the lower part on the whole. We attribute this result to relative low crystalline quality in the upper part.

The PL properties of the arrays with different erosion times were characterized as shown in Fig. 5. It can be indicated that ZnO exhibits mainly two PL bands located at UV and visible wavelengths, corresponding band-gap emission and defect-related emission, respectively. It can be observed clearly from Fig. 5 that the intensity of the band gap emission becomes weaker while the defects emission becomes stronger as the erosion time extends. The reason assigned for decrease in band-to-band emission may be due to the surface state defects induced by etching and sample consumption. Some photons radiated from band to band may be absorbed during emitting by the surface defects. With the increase of etching time, the surface defects increase and more photons were absorbed. Therefore, the intensity of band emitting decreases with the etching time. Chemical etching is an efficient way to induce defects which has been used to tailor crystal properties [32,33]. In this case, the etching rate for zinc and oxygen atoms on the ZnO microrod surface may be different, thus the introducing of surface state defect is quite possible. Børseth et al. indicated a V_O (O vacancy) related defect level at around 2.53 eV (~475 nm) and a V_{Zn} (Zn vacancy) related defect level at around 2.35 eV (~510 nm) in the visible spectrum in single crystal ZnO [34]. However, in this work, the increase of structure defects is unlikely during erosion process. Therefore, the rise of the defect emission should be explained by the increase of surface states rather than vacancy defects.

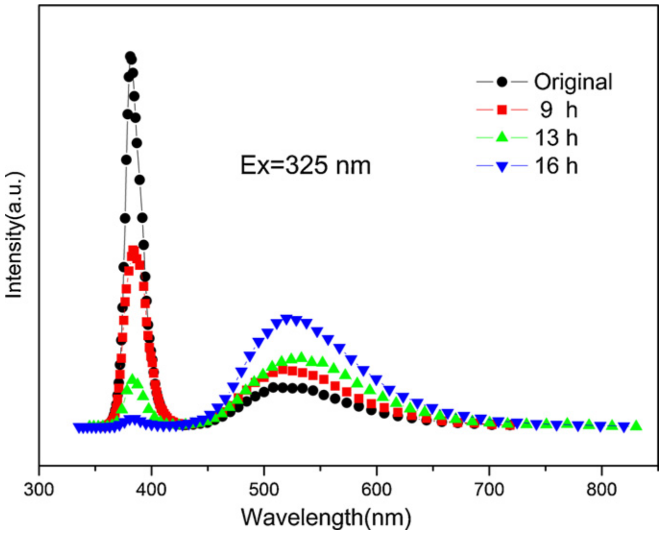

Fig. 5. PL properties of ZnO microrod arrays with different erosion times.

4. Conclusion

Large-area highly oriented ZnO microrod arrays were successfully deposited on 6H–SiC substrate by a facile CVD method. PL intensities between band gap emission and defect-related emission can be tuned by acid etching for varying durations. The intensity of the band gap emission becomes weaker while the defects emission becomes stronger as the erosion time extends. This provides a potential way to control the PL properties of ZnO materials and possibly shed light on the mechanism of PL in semiconductors.

Acknowledgement

This work is supported by the National Basic Research Program of China (973 Program) grant No. 2007CB936300.

References

[1] C.J. Lee, T.J. Lee, S.C. Lyu, Y. Zhang, H. Ruh, H.J. Lee, Appl. Phys. Lett. 81 (2002) 3648.
[2] M.H. Huang, S. Mao, H. Feick, H. Yan, Y. Wu, H. Kind, E. Weber, R. Russo, P. Yang, Science 292 (2008) 1897.
[3] L. Vayssieres, K. Keis, S.-E. Lindquist, A. Hagfeldt, J. Phys. Chem. B 105 (2001) 3350.
[4] L. Vayssieres, K. Keis, A. Hagfeldt, S.-E. Lindquist, Chem. Mater. 13 (2001) 4395.
[5] R. Liu, A.A. Vertegel, E.W. Bohannan, T.A. Sorenson, J.A. Switzer, Chem. Mater. 13 (2001) 508.
[6] M. Matsuu, S. Shimada, K. Masuya, S. Hirano, M. Kuwabara, Adv. Mater. 18 (2006) 1617.
[7] X.D. Wang, C.J. Summers, Z.L. Wang, Nano Lett. 4 (2004) 423.
[8] J. Rybczynski, D. Banerjee, A. Kosiorek, M. Giersig, Z.F. Ren, Nano Lett. 4 (2004) 2037.
[9] D.F. Liu, Y.J. Xiang, X.C. Wu, Z.X. Zhang, L.F. Liu, L. Song, X.W. Zhao, S.D. Luo, W.J. Ma, J. Shen, W.Y. Zhou, G. Wang, C.Y. Wang, S.S. Xie, Nano Lett. 6 (2006) 2375.
[10] Y.J. Kim, C.H. Lee, Y.J. Hong, G.C. Yi, Appl. Phys. Lett. 89 (2006) 163128.
[11] S. Xu, Y.G. Wei, M. Kirkham, J. Liu, W.J. Mai, D. Davidovic, R.L. Snyder, Z.L. Wang, J. Am. Chem. Soc. 130 (2008) 14958.
[12] W.I. Park, G.C. Yi, M.Y. Kim, S.J. Pennycook, Adv. Mater. 14 (2002) 1841.
[13] W.I. Park, G.C. Yi, J.W. Kim, S.M. Park, Appl. Phys. Lett. 82 (2003) 4358.
[14] G. Meng, X.D. Fang, Y.K. Zhou, J. Seo, W.W. Dong, S. Hasegawa, H. Asahi, H. Tambo, M.G. Kong, L. Li, J. Alloys Compd. 491 (2010) 72.
[15] Q.X. Zhao, M. Willander, R.E. Morjan, Q.H. Hu, E.E.B. Campbell, Appl. Phys. Lett. 83 (2003) 165.
[16] H.T. Ng, J. Han, T. Yamada, P. Nguyen, Y.P. Chen, M. Meyyappan, Nano Lett. 4 (2004) 1247.
[17] J.H. He, C.S. Lao, L.J. Chen, D. Davidovic, Z.L. Wang, J. Am. Chem. Soc. 127 (2005) 16376.
[18] W.J. Mai, P.X. Gao, C.S. Lao, Z.L. Wang, A.K. Sood, D.L. Polla, M.B. Soprano, Chem. Phys. Lett. 460 (2008) 253.
[19] H. Zhang, L. Wang, H. Xiong, L. Hu, B. Yang, W. Li, Adv. Mater. 15 (2003) 1712.
[20] N. Gaponik, I.L. Radtchenko, G.B. Sukhorukov, H. Weller, A.L. Rogach, Adv. Mater. 14 (2002) 879.
[21] Y.F. Chen, Z. Rosenzweig, Nano Lett. 2 (2002) 1299.
[22] C.Y. Tan, M.R. Pinto, K.S. Schanze, Chem. Commun. (2002) 446.
[23] G.A. Montano, A.M. Dattelbaum, H.L. Wang, A.P. Shreve, Chem. Commun. (2004) 2490.
[24] A.L. Pan, H. Yang, R.B. Liu, R.C. Yu, B.S. Zou, Z.L. Wang, J. Am. Chem. Soc. 127 (2005) 15692.
[25] X. Tang, E. Choo, L. Li, J. Ding, J. Xue, Chem. Mater. 22 (2010) 3383.
[26] A.L. Pan, L. Yao, Y. Qin, Y. Yang, D.S. Kim, R. Yu, B. Zou, P. Werner, M. Zacharias, U. Gösele, Nano Lett. 8 (2008) 3413.
[27] D. Wang, G. Xing, H. Peng, T. Wu, J. Phys. Chem. C 113 (2009) 7065.
[28] H.M. Xiong, Z.D. Wang, D.P. Liu, J.S. Chen, Y.G. Wang, Y.Y. Xia, Adv. Funct. Mater. 15 (2005) 15.
[29] H. Zhao, L. Dai, M. Zhao, Y. Xu, X.L. Chen, J. Alloys Compd. 416 (2006) 315.
[30] W. Cheng, P. Wu, X. Zou, T. Xiao, J. Appl. Phys. 100 (2006) 054311.
[31] A. Wander, F. Schedin, P. Steadman, A. Norris, R. McGrath, T.S. Turner, G. Thornton, N.M. Harrison, Phys. Rev. Lett. 86 (2001) 3811.
[32] W. Jost, J. Weber, H. Lemke, Semicond. Sci. Technol. 11 (1996) 22.
[33] M. Yoneta, Y. Kamiura, F. Hashimoto, Phys. Status Solidi (2003) 635, 0.
[34] M.T. Børseth, B.G. Svensson, A.Y. Kuznetsov, Appl. Phys. Lett. 89 (2006) 262112.